ORIGINAL ARTICLE

Comparing diagnostic accuracy of ^{18}F-FDG-PET/CT, contrast enhanced CT and combined imaging in patients with suspected vascular graft infections

Lars Husmann[1] · Martin W. Huellner[1] · Bruno Ledergerber[2] · Alexia Anagnostopoulos[2] · Paul Stolzmann[1] ·
Bert-Ram Sah[1,3,4] · Irene A. Burger[1] · Zoran Rancic[5] · Barbara Hasse[2] · and the Vasgra Cohort

Abstract

Background To evaluate the diagnostic accuracy of positron emission tomography/computed tomography with ^{18}F-fluorodeoxyglucose (PET/CT), contrast-enhanced CT (CE-CT), and a combined imaging approach (CE-PET/CT) in patients with suspected vascular graft infection (VGI).

Methods PET/CT and CE-CT were performed prospectively in 23 patients with suspected VGI. Diagnostic accuracy for PET/CT was assessed by using previously suggested cut-off points for maximum standardized uptake values (SUV_{max}) measured in the vicinity of the graft. Using a new 4-point scale for visual grading, two readers independently assessed the diagnostic accuracy for CE-CT and combined CE-PET/CT. Microbiological culture, obtained after open biopsy or graft explantation, and clinical follow-up of the patients served as the standard of reference.

Results Sensitivity, specificity, negative predictive value (NPV), positive predictive value (PPV), and accuracy of PET/CT for the diagnosis of VGI was 100%, 50%, 100%, 72.2%, and 78.3%, using the most favorable SUV_{max} cut-off ≥ 4.9. Respective values for CE-CT were 100%, 50%, 100%, 72.2%, and 78.3% for reader 1, and 92.3%, 80%, 88.9%, 85.7%, and 86.9% for reader 2; while respective values for combined CE-PET/CT were 100%, 70%, 100%, 81.3%, and 86.9% for reader 1, and 100%, 80%, 100%, 86.7%, and 91.3% for reader 2. Additionally, imaging provided a conclusive clinical diagnosis in patients without graft infection (i.e., other sites of infection): five of ten patients with CE-CT, six of ten patients with PET/CT, and seven of ten patients with combined CE-PET/CT.

Conclusion The diagnostic accuracy of combined CE-PET/CT in patients with suspected VGI is very high. The combination of the high sensitivity of PET/CT in detecting metabolically active foci in infection, and the high specificity of CE-CT in detecting anatomic alterations, appears to be the reason why combined imaging outperforms stand-alone imaging in diagnosing VGI and may be supportive in future decision-making of difficult cases of suspected VGI.

Clinical Trials.gov Identifier: NCT01821664.

✉ Lars Husmann
lars.husmann@usz.ch

1   Department of Nuclear Medicine, University Hospital of Zurich / University of Zurich, Raemistrasse 100, CH-8091 Zurich, Switzerland

2   Division of Infectious Diseases and Hospital Epidemiology, University Hospital of Zurich / University of Zurich, Raemistrasse 100, CH-8091 Zurich, Switzerland

3   Institute of Diagnostic and Interventional Radiology, Department Medical Radiology, University Hospital of Zurich / University of Zurich, Raemistrasse 100, CH-8091 Zurich, Switzerland

4   Department of Cancer Imaging, King's College London, London, UK

5   Clinic for Cardiovascular Surgery, University Hospital of Zurich / University of Zurich, Raemistrasse 100, CH-8091 Zurich, Switzerland

Introduction

Vascular graft infections (VGI) are associated with a high mortality and morbidity risk [1–3], and require an immediate and definite diagnosis [4, 5]. An initial report on the diagnostic accuracy of ^{18}F-fluorodeoxyglucose (FDG) positron emission tomography/computed tomography (PET/CT) for VGI diagnosis reported a higher accuracy of PET/CT compared to contrast-enhanced computed tomography (CE-CT) [6]. Subsequent studies confirmed the higher accuracy of PET/CT in the detection of VGI [7–11], yet comparative data are scarce, and often hampered by the heterogeneity of patient populations and the variability of imaging protocols and time points of imaging [6–11].

In CE-CT, diagnostic imaging criteria for VGI are fat-stranding, fluid collection, contrast enhancement, and gas formation in the vicinity of the vascular graft. PET/CT, on the other hand, detects FDG-avid lesions adjacent to the vascular graft, since FDG accumulates in metabolically active cells and thus detects inflammatory processes [12, 13]. Hence, using PET/CT, VGI may be detected earlier; in less severe stages; lower grade infection may also be detected. However, false positive PET/CT studies due to foreign body reactions or postoperative tissue formation [14–16], have been reported, hampering the specificity of the imaging modality [6–11, 16]. To date, potential advantages of a combined imaging approach of PET/CT and CE-CT (combined CE-PET/CT), as routinely performed in many oncologic imaging studies [17], have only rarely been assessed in the literature [9, 18] . Therefore, the aim of the present study was to assess the diagnostic accuracy of PET/CT, CE-CT, and combined CE-PET/CT in a well-defined prospective cohort of patients with suspected VGI, using microbiologic results and clinical follow-up as the standard of reference. Furthermore, we aimed to assess and compare readers' confidence in their CE-PET/CT and CE-CT findings.

Material and methods

Study design and data collection

We included participants of the Vascular Graft Cohort Study (VASGRA; clinical trials. Gov identifier: NCT01821664) with suspected VGI in this analysis. Patients aged 18 years or older with any type of vascular graft operation since November 2012 are included in the cohort und a systematic follow-up is performed. The institutional review board approved the study, and we obtained written informed consent from all participants (KEK-ZH-Nr. 2012–0583).

We used the Management of Aortic Graft Infection Collaboration (MAGIC) criteria for VGI diagnosis [5]. A multi-disciplinary team of infectious disease specialists, cardiovascular surgeons, radiologists, nuclear medicine physicians, and microbiologists adjudicated every clinical case. Gold standard for VGI diagnosis was a positive microbiological culture of the deep tissue around the vascular prosthesis, obtained by open biopsy or a positive microbiological culture of an explanted vascular graft. Clinical, laboratory, histopathological, and imaging results were also taken into account, serving as the standard of reference in cases with excluded VGI. In equivocal cases, follow-up was performed. As per protocol, patients with suspected VGI received a combined CE-PET/CT either prior to treatment or as soon as possible after the start of antimicrobial treatment. We excluded images of patients with emergency re-do surgery before radiological examination or patients with images obtained > 3 months after VGI diagnosis.

PET and CT data acquisition

Patients fasted for at least 4 hours and had no insulin injections 4 hours prior to FDG administration. Body weight, height, and blood glucose level were measured prior to injection of FDG. In non-diabetic patients a blood glucose level of < 8 mmol/l, and in diabetic patients a blood glucose level of <11 mmol/l, was accepted for imaging. After intravenous injection of body weight-adapted FDG (358 megabecquerels [Interquartile range, (IQR) 326–394], patients were resting for a standardized uptake time of 60 minutes. Imaging data were acquired with the patient in supine position with arms overhead. We used a Discovery VCT (GE Healthcare) for PET/CT and CE-CT until December 2016, and thereafter switched to a Discovery MI (GE Healthcare) for the remaining scans. Both PET/CT systems used non-enhanced CT scans for attenuation correction. We performed scans from the vertex of the skull to the mid-thigh level, with a tube voltage of 120–140 kV and a tube current–time product of 10–100 mAs. CT data for attenuation correction and anatomic reference were reconstructed with a slice thickness of 3.75 mm and an increment of 3.0 mm. PET scans with the Discovery VCT were acquired using the 3-dimensional mode with a fixed scan duration of 2 minutes per bed position, while scans with the Discovery MI were acquired using a time-of-flight mode with a fixed scan duration of 2.5 min per bed position.

CE-CT was performed of the chest and/or abdomen, depending on the location of the vascular graft. After intravenous injection of 80 ml of iodinated contrast material (Visipaque® 320, GE Healthcare), CE-CT was timed for imaging at arterial (threshold-based initiation using a region of interest in the aorta) and portal venous phase (50 s after the arterial phase) with a tube voltage of 120 kV and a tube current–time product of 100–320 mAs.

Image analysis

All data sets (PET/CT, CE-CT, combined CE-PET/CT) were independently analysed by two experienced and double board

certified radiologists and nuclear medicine physicians on a AW Workstation Version 4.6 (GE Healthcare Biosciences, Pittsburgh, PA, USA). Readers were blinded to all clinical patient data, except the date of the examination as well as the date of the index operations. All data sets were analyzed for secondary diagnoses (i.e., infectious foci not in the vicinity of a graft or other relevant findings, such as malignancy). Results were presented according to the standards for reporting of diagnostic accuracy (STARD).

PET/CT

Readers determined whether focal or diffuse FDG uptake was present along the vascular graft [10]. If focal uptake was detected, readers measured the maximum standardized uptake value (SUV_{max}) with the use of an in-built software. For the latter, a volume-of-interest (VOI) was placed on the site of highest FDG uptake in the wall of the vascular graft or native aorta, and SUV_{max} was subsequently measured as the hottest voxel within the given VOI. The correct placement of the VOI in the strongest focus of FDG activity was confirmed by the use of axial, coronal, and sagittal reformatted images in order to avoid partial-volume effects or signal spillover from neighboring organs such as the kidney. Four different cut-off values were used to determine the presence of VGI with PET/CT and to calculate diagnostic performances. Three of these cut-offs were previously suggested in the literature: (i) $SUV_{max} \geq 3.8$ [10], (ii) $SUV_{max} \geq 4.9$ [10], and (iii) $SUV_{max} \geq 8$ [11]. The fourth ($SUV_{max} >$ liver uptake) was introduced on the basis of clinical routine in oncologic imaging [19].

CE-CT and combined CE-PET/CT

Readers determined whether a VGI was present or not; notably, no cut-offs were defined (i.e., for SUV measurements) and no single imaging criteria (i.e., fluid collection, or contrast enhancement) was considered to be essential for the final diagnosis. Differences between the two readers were analyzed, but no consensus reading was performed. Furthermore, both readers scored their confidence in their diagnosis, using a 4-point score (adapted for both imaging modalities as described below). Scores 1 and 2 were considered negative for infection, while scores 3 and 4 were considered positive for VGI. To determine the level of confidence of the readers in their own diagnosis, we defined scores 1 and 4 as "confident" and scores 2 and 3 as "not confident"; the rate of "confident" and "non-confident" findings was calculated for each reader and each method. Additionally, readers of CE-CT were asked to document the presence or absence of the following imaging findings: fat stranding, fluid collection, contrast enhancement, and gas formations.

CE-CT Score: Score 1: no signs for VGI. Score 2: most likely post-interventional changes and no VGI. Score 3:

suspicion of VGI. Score 4: clear signs for VGI. *Combined CE-PET/CT score:* Score 1: no signs for VGI. Score 2: most likely foreign body reaction (i.e., diffuse FDG uptake along the graft) and/or post interventional changes and no VGI. Score 3: suspicion of VGI. Score 4: clear signs of VGI.

Statistical analyses

Variables were expressed as median and interquartile range (IQR; 25th, 75th percentiles) or percentages. Sensitivity, specificity, negative predictive values (NPV), positive predictive values (PPV), and accuracy were determined for the diagnosis of VGI for all readers of all imaging modalities (i.e., PET/CT, CE-CT, and combined CE-PET/CT), as well as for the presence of imaging fingings in CE-CT (fat stranding, fluid collection, contrast enhancement, gas formations, and the combined presence of all four), and finally, for both readers with and without confidence in their diagnosis, using a 4-point scale considering the criteria as described in the method section above. Measures were complemented with binomial 95% confidence intervals. For PET/CT, we determined the SUV_{max} cut-point at the receiver operator curve (ROC) yielding the highest accuracy of VGI diagnosis in our study population. An area under the ROC curve of 0.5–0.6 was rated as 'failed', 0.6–0.7 as 'poor', 0.7–0.8 'fair', and 08.-1.0 as 'good'. Fisher's exact tests were used to determine significant differences in diagnostic accuracy between readers and methods, and to determine the association of reader's confidence and diagnostic accuracy. Wilcoxon signed-rank tests were used to determine differences in SUV_{max} between infected and non-infected grafts. A *P* value of < .05 was considered to indicate statistical significance. Statistical analysis was performed using commercially available software (Stata/SE, Version 15.1, StataCorp, College Station, TX, USA).

Results

Patient population

PET/CT combined with CE-CT was successfully performed with diagnostic image quality in 59 patients with suspected VGI. Thereof, imaging results of 36 participants were excluded due to PET/CT imaging > 3 months after VGI diagnosis or VGI exclusion (*n* = 22), imaging patients with no graft, but mycotic aneurysm (*n* = 2), imaging after installation of negative pressure wound therapy or re-do surgery (*n* = 6), missing follow up (*n* = 1), or missing key variables (n = 6). The final study population consisted of 23 patients. Patient demographics are displayed in Table 1. Fourteen patients (61%) did not receive any antibiotic treatment prior to PET/CT, while in nine patients (31%) antibiotic treatment was already started [median 11 days (range 3–16)] prior to imaging.

Table 1 Baseline characteristics

	All	VGI	No VGI
Number of patients, n (%)	23(100)	13(57)	10(43)
Age, median years (IQR)	65 (60–72)	61 (61–66)	69 (58–77)
Male gender, n (%)	23 (100)	13 (100)	10 (100)
Diabetes mellitus, n (%)	4 (17)	3 (23)	1 (25)
Glucose level at time of imaging, median mmol/l (IQR)	5.5 (5.2–5.8)	5.3 (5.0–5.9)	5.5 (5.3–5.8)
C-reactive protein at time of imaging, median mg/l (IQR)	75 (40–129)	90 (56–217)	65 (40–94)
Type of index operation			
Aortic arch replacements, n (%)	12(52)	7(54)	5(50)
Aorto-biiliac grafts, n (%)	8(35)	4(31)	4(40)
Thoracic endovascular aortic repair, n (%)	3(13)	2(15)	1(10)
Type of graft			
Biograft/ Dacron, n (%)	2(8.7)	1(7.7)	1(10)
Dacron, n (%)	8(35)	4(31)	4(40)
Dacron/ polytetrafluoroethylene, n (%)	1(4.3)	0(0)	1(10)
Polytetrafluoroethylene, n (%)	8(35)	4(31)	4(40)
Pyrolytic carbon/ Dacron, n (%)	4(17)	4(31)	0(0)
Days between index operation and imaging, median days (IQR)	243 (63–644)	392 (211–644)	160 (62–575)

VGI: vascular graft infection; IQR, interquartile range

Thirteen patients (57%) had VGI (Fig. 1), while VGI was ruled out in the remaining ten patients (43%) (Figs. 2, 3, and 4). Final diagnosis for the ten patients for whom VGI was excluded were: pneumonia ($n = 3$), sternal wound infection and spondylodiscitis ($n = 1$), Dressler syndrome ($n = 2$), diverticulitis ($n = 1$), gout ($n = 1$), retroperitoneal fibrosis with consecutive ureteral obstruction ($n = 1$), and sinusitis ($n = 1$). Whole-body PET/CT correctly identified six of these conditions: pneumonia ($n = 2$), sternal wound infection and spondylodiscitis ($n = 1$), diverticulitis ($n = 1$), retroperitoneal fibrosis with consecutive ureteral obstruction ($n = 1$), and sinusitis ($n = 1$), while CE-CT correctly identified five findings: pneumonia ($n = 3$), sternal wound infection and spondylodiscitis ($n = 1$), retroperitoneal fibrosis with consecutive ureteral obstruction ($n = 1$). Combined CE-PET/CT identified seven conditions: pneumonia ($n = 3$), sternal wound infection and spondylodiscitis ($n = 1$), retroperitoneal fibrosis with consecutive ureteral obstruction ($n = 1$), and sinusitis ($n = 1$), and diverticulitis ($n = 1$).

Diagnostic performance of PET/CT

Both readers found an increased focal FDG uptake in the same 19 patients (83%) and no increased uptake in the same three remaining patients (13%). In one patient (4%), one reader diagnosed no increased uptake, while the other diagnosed diffusely increased uptake. In 6/23 cases (26%), SUV_{max} measurements at the graft differed between the two readers and a consensus reading was performed, which served for further analysis. Median SUV_{max} values in all vascular grafts were 7.1 (IQR 5.1–8.5), while median SUV_{max} values were higher in patients with proven VGI than in patients with no infected grafts [8.3 (7.6–9.4) vs 4.9 (3.6–6.4); $P < 0.001$]. ROC analysis provided an area under the curve (AUC) of 0.86; hence, an SUV_{max} of ≥ 6.5 was determined as a cut-off value to differentiate between infected and non-infected grafts (92% sensitivity and 80% specificity) for the present patient population.

SUV_{max} measurements in the liver differed in 21/23 cases (91%), with the largest difference in SUV_{max} between readers being at 0.6. Therefore, we decided to calculate the average SUV_{max} for each patient for further analyses [3.5 (95% confidence interval (CI) 3.3–3.8)]. Diagnostic performances of PET/CT using four different cut-off values (i.e. ≥ 3.8, ≥ 4.9, ≥ 8, and > liver uptake) are displayed in Table 2. The highest diagnostic accuracy was achieved using an SUV_{max} cut-off value of ≥ 4.9. However, there was no statistically significant difference between the cut-offs (all $P > 0.3$).

Diagnostic performance of CE-CT

Diagnostic performance of CE-CT for both readers and all imaging findings is displayed in Table 2. Diagnostic accuracy did not significantly differ between readers ($P = 0.7$), and was higher when readers were confident in their diagnosis. However, the latter was not statistically significant ($P = 1.0$ for reader 1, and $P = 0.09$ for reader 2). The detection rate of the imaging findings (fat stranding, fluid collection, contrast enhancement, gas formations) differed little between readers 1 and 2 (19 vs 18 for fat stranding;
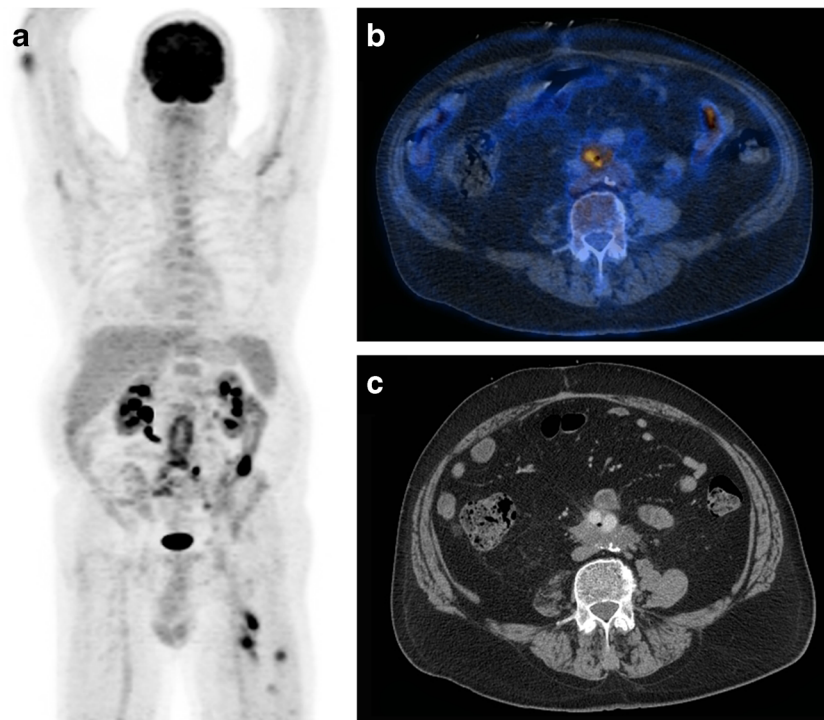
Fig. 1 A 65-year-old man with a history of an open aorto-biiliac reconstruction presented with fever, chills, and weight loss. He was diagnosed with vascular graft infection caused by an enteroaortic fistula. Due to COPD Gold IV, he was assessed as being inoperable. In a multiple-staged approach, the patient underwent emergency endovascular aortic repair, resection of the aortoenteric fistula followed by local debridements, and negative pressure wound therapy. At the time of diagnosis, maximum intensity reconstructions of PET (**a**) and fused PET/CT images (**b**) showed strongly increased FDG uptake along the aorto-biiliac aortic repair, which appeared mostly focal (**a** and **b**). All readers of PET/CT, CE-CT, combined CE-PET/CT rated the examination true positive. Both CE-CT readers described perigraft fat stranding, soft-tissue enhancement, and fluid and gas formation (**c**). As an incidental finding, septic emboli in the left upper leg were diagnosed on PET images (**a**)

20 vs 20 for fluid collections; 16 vs 17 for contrast enhancement; 6 vs 4 for gas formations; and 4 vs 3 for the combination of all four imaging findings). The imaging finding "fat stranding" displayed the highest diagnostic accuracy for both readers (74% and 78%); however, differences between stand-alone imaging findings in diagnostic accuracy were not significant ($P = 1.0$ reader 1; $P = 0.12$ reader 2). Notably, a perfect sensitivity of 100% was detected with the imaging finding "fat stranding", while a perfect specificity of 100% was obtained with the combination of all four imaging findings (same results for both readers).

Diagnostic performance of combined CE-PET/CT

Diagnostic performance of combined CE-PET/CT for both readers is displayed in Table 2. Diagnostic accuracy did not significantly differ between readers ($P = 1.0$). Using the SUV_{max} cut-offs ≥ 3.8, ≥ 4.9, ≥ 8, and > liver true-positive findings were detected in 13, 13, 8, and 13 PET/CTs respectively. The detection rates of the 13 VGIs were also high in CE-CT (reader 1, $n = 13$; reader 2, $n = 12$) and combined CE-PET/CT (both readers, $n = 13$).

Diagnostic findings of PET/CT, CE-CT and CE-PET/CT

True-negative PET/CT findings were detected at the following SUV_{max} cut-offs: ≥ 3.8 ($n = 3$), ≥ 4.9 ($n = 5$), ≥ 8 ($n = 9$), and > liver ($n = 0$). With the use of CE-CT, true-negative VGI were identified in five and eight instances for reader 1 and reader 2 respectively. Combined CE-PET/CT excluded VGI diagnosis in seven (reader 1) and eight cases (reader 2). Five false-negative PET/CT findings occurred at an SUV_{max} cut-off of ≥ 8, whereas in CE-PET/CT no false negative findings occurred. False-positive PET/CT findings were found at an SUV_{max} cut-off of ≥ 3.8, ≥ 4.9, ≥ 8, and > liver in seven, five, one, and nine PET/CTs respectively. CE-CT detected five (reader 1) and two (reader 2) false-positive VGI. Notably, the lowest rate of false-positive findings was detected with combined CE-PET/CT: $n = 3$ (reader 1), and $n = 2$ (reader 2). The respective vascular graft types for false-positive findings in combined CE-PET/CT were Biograft combined with Dacron and Dacron combined with polytetrafluoroethylene (both readers) and Dacron (reader 1). The respective time intervals after the index operation for false-positive findings were 136 and 781 days (both readers) and 145 days (only
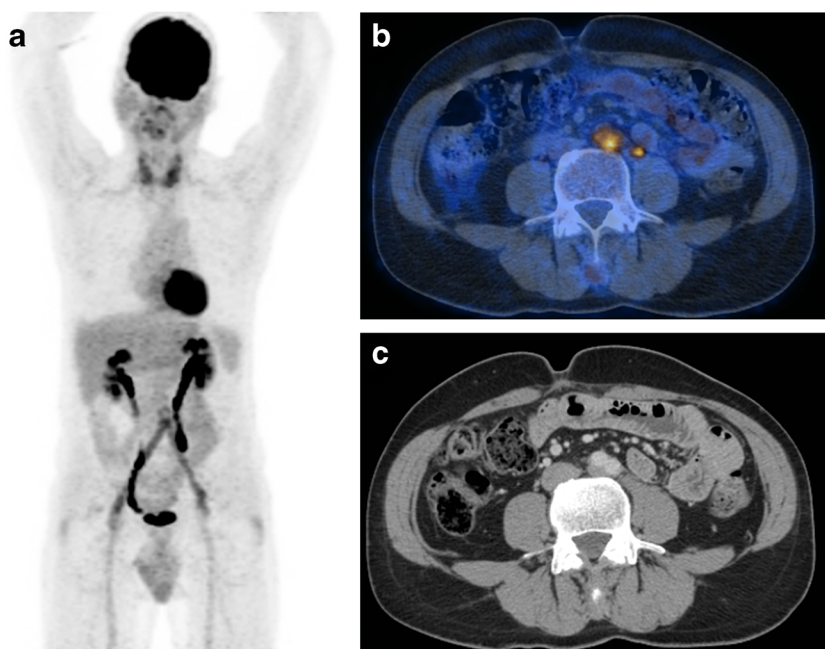
Fig. 2 A 53-year-old male patient with a history of an open aortic reconstructive surgery presented with belt-shaped pain without fever. A VGI was excluded, and instead a retroperitoneal fibrosis with subsequent obstruction of the ureter was diagnosed. Maximum intensity reconstructions of PET (**a**) and fused PET/CT images (**b**) showed increased FDG uptake along the entire aorto-biiliac aortic reconstruction, which appeared focally increased at the bifurcation (**a** and **b**). Both PET readers rated the examination false positive for VGI (scores 3 and 4). Also, both readers of CE-CT rated the examination false positive; both described perigraft fat stranding, one reader additionally described soft-tissue enhancement (**c**). With combined CE-PET/CT, both readers rated the examination true negative, both stating however, not to be confident in their diagnosis (score 2). As an incidental finding, metabolically active thyroiditis was diagnosed on PET images and subsequently confirmed clinically (**a**)

reader 1), two time intervals (136 and 145) being below the median, and one (781) being above (Table 1).

Reader's confidence in their diagnosis

CE-CT: Reader 1 was confident in 11 cases (44%), while reader 2 was confident in 12 cases (48%). *Combined CE-PET/CT:* Reader 1 was confident in 17 cases (74%), while reader 2 was confident in 15 cases (65%). Confidence in combined CE-PET/CT did not significantly differ between readers ($P = 1.0$), but was higher as compared to stand-alone CE-CT ($P = 0.13$ for reader 1; $P = 0.24$ for reader 2; Table 2). Higher reader's confidence was associated with higher diagnostic accuracy, however, not statistically significant (p = 1.0 for both readers; Table 2).

Discussion

We prospectively assessed patients with vascular graft infections (VGIs) and studied the diagnostic accuracy of CE-CT and combined CE-PET/CT for VGI diagnosis. We investigated 13 prospective patients with VGI and 10 patients without VGI. In our study combined imaging with CE-CT and PET/CT yielded a higher diagnostic accuracy than stand-alone imaging. The highest confidence of readers in their imaging diagnosis was found with combined imaging – while reader's confidence was associated with higher diagnostic accuracy. When SUV$_{max}$ cut-off values were used to determine the presence of VGI in stand-alone PET/CT, the diagnostic accuracy was lower as compared to stand-alone CE-CT and combined CE-PET/CT.

Accuracy of stand-alone PET/CT

Previous publications suggested the use of SUV$_{max}$ cut-offs for the diagnosis of VGI with PET/CT [8, 10, 11]. In the present study, the highest diagnostic accuracy for stand-alone PET/CT was found, using a SUV$_{max}$ cut-off of ≥4.9 for focal lesions adjacent to the graft. However, the diagnostic accuracy in our study was lower as compared to previous publications (i.e. 78% vs. 84–94% [6, 8]), yielding a very high sensitivity of 100%, but a low specificity of only 50%. In contrast to previous publications, the diagnostic accuracy of stand-alone PET/CT in our study was even lower than that of stand-alone CE-CT in the present study. Thus, we suggest to either refrain from using of SUV$_{max}$ cut-off values, or to use them with caution and only as an adjunct to other imaging-derived information, when stand-alone imaging with PET/CT is
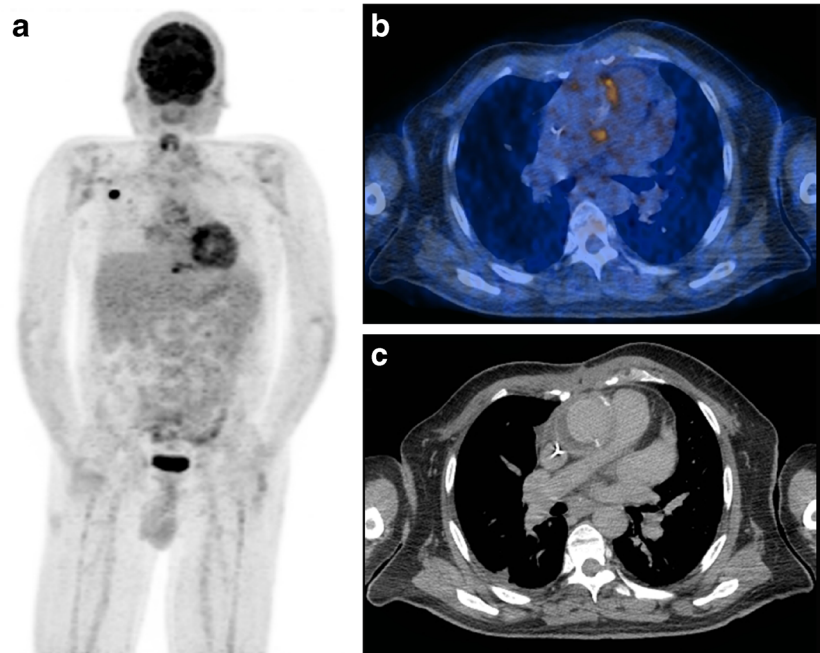
Fig. 3 A 50-year-old male patient received emergency supracoronary and aortic arch repair for thoracic aortic dissection. Four weeks later, the febrile patient presented with redness, and swelling of the distal sternum and back pain. With positive blood cultures for *Staphylococcus epidermidis*, a sternal wound infection was diagnosed. The patient underwent sternal revision, debridement, and negative pressure wound therapy. Despite a fluid collection adjacent to the vascular graft, the clinical team excluded VGI since intraoperative culture results (swab from graft and perigraft tissue) were negative. Follow-up PET/CT scan showed a diffuse tracer uptake of the vascular graft, which was interpreted as foreign body reaction and the patient recovered well without any signs of VGI to date (follow-up time 2 years). As an explanation for his back pain, spondylodiscitis was diagnosed (refer to Fig. 4). Maximum intensity reconstructions of PET (**a**) and fused PET/CT images (**b**) showed focally increased FDG-uptake along the thoracic aortic repair (**a** and **b**). Both PET readers rated the examination false positive for VGI (score 3). One CT reader rated the examination false positive, the other true negative — both described perigraft fat stranding and fluid formation, while one additionally described soft-tissue enhancement (**c**). With combined CE-PET/CT, one reader rated the examination false positive, the other true negative — both stated, not to be confident in their diagnosis (score 2 and 3)

performed to diagnose VGI. Our suggestion is in line with findings of a comparable and recent publication on infectious endocarditis [20] and also VGI [18], in which metabolic cut-off values failed to accurately determine infection [20].

Accuracy of stand-alone CE-CT

The diagnostic accuracy of CE-CT in our study was high, and comparable to previous studies (79%–100% [6, 13, 18] vs 78 and 87% in the present study). We also calculated diagnostic performances of stand-alone CT criteria, displaying large ranges of sensitivities (23.1–100%) and specificities (30.0–100%), which is in line with the study from Saleem et al. on 23 patients with VGI [18]. Notably, when all four imaging criteria (fat stranding, fluid collection, contrast enhancement, and gas formations) were detected simultaneously, the specificity of CE-CT was 100%. The latter, may account for the fact, that combined imaging outperforms stand-alone imaging modalities in the diagnosis of VGI, as CE-CT adds specificity to the highly sensitive PET/CT, resulting in an improved diagnostic accuracy.

Accuracy of combined CE-PET/CT

Combined imaging using CE-CT and PET/CT yielded higher diagnostic accuracy than stand-alone imaging in the present study. A combined imaging approach for the diagnosis of VGI has been investigated in a previous studie [9], and in this particular study combined CE-PET/CT and stand-alone PET/CT performed with similar diagnostic accuracy, while both imaging modalities outperformed stand-alone CE-CT. However, in line with a comparable study on infectious endocarditis [20], we found that stand-alone PET/CT has a high sensitivity, but a low specificity in detecting infectious foci, while CE-CT displays a higher specificity but lower sensitivity, and the combination of both methods results in the best diagnostic performance [20]. In the same study, Pizzi et al. also described a reduced rate of doubtful cases with combined imaging, which is also in line with our findings, as we describe the highest reader's confidence with combined imaging, and demonstrate that high reader's confidence is associated with high diagnostic accuracy.

Table 2 Diagnostic accuracy of PET/CT, CE-CT, combined CE-PET/CT

|	Sensitivity % (95% CI)	Specificity % (95% CI)	NPV % (95% CI)	PPV % (95% CI)	Accuracy % (95% CI)
PET/CT					
SUV max. cut-off ≥ 3.8	100(75.3–100)	30.0(6.7–65.2)	100(29.2–100)	65.0(40.8–84.6)	69.6(47.1–86.8)
SUV max. cut-off ≥ 4.9	100(75.3–100)	50.0(18.7–81.3)	100(47.8–100)	72.2(46.5–90.3)	78.3(56.3–92.5)
SUV max. cut-off ≥ 8	61.5(31.6–86.1)	90.0(55.5–99.7)	64.3(35.1–87.2)	88.9(51.8–99.7)	73.9(51.6–89.8)
SUV max. cut-off ≥ liver	100(75.3–100)	10.0(0.3–44.5)	100(2.5–100)	59.1(36.4–79.3)	73.9(51.6–89.8)
CE-CT					
Reader 1 overall	100(75.3–100)	50.0(18.7–81.3)	100(47.8–100)	72.2(46.5–90.3)	78.3(56.3–92.5)
– If confident	100(63.1–100)	33.3(0.8–90.6)	100(2.5–100)	80.0(44.4–97.5)	81.8(48.2–97.7)
– If not confident	100(47.8–100)	57.1(18.4–90.1)	100(39.8–100)	62.5(24.5–91.5)	75.0(42.8–94.5)
– Fat stranding	100(75.3–100)	40.0(12.2–73.8)	100(39.8–100)	68.4(43.4–87.4)	73.9(51.6–89.8)
– Fluid collection	100(75.3–100)	30.0(6.7–65.2)	100(29.2–100)	65.0(40.8–84.6)	69.6(47.1–86.8)
– Contrast enhancement	84.6(54.6–98.1)	50.0(18.7–81.3)	71.4(29.0–96.3)	68.8(41.3–89.0)	69.6(47.1–86.8)
– Gas formations	46.2(19.2–74.9)	100(69.2–100)	58.8(32.9–81.6)	100(54.1–100)	69.6(47.1–86.8)
– All four findings present	30.8(9.1–61.4)	100(69.2–100)	52.6(28.9–75.6)	100(39.8–100)	60.9(38.5–80.3)
Reader 2 overall	92.3(64.0–99.8)	80.0(44.4–97.5)	88. (51.8–99.7	85.7(57.2–98.2)	86.9(66.4–97.2)
– If confident	100(69.2–100)	100(15.8–100)	100(15.8–100)	100(69.2–100)	100(73.5–100)
– If not confident	66.7(9.4–99.2)	75.0(34.9–96.8)	85.7(42.1–99.6)	50.0(6.8–93.2)	72.7(39.0–93.9)
– Fat stranding	100(75.3–100)	50.0(18.7–81.3)	100(47.8–100)	72.2(46.5–90.3)	78.3(56.3–92.5)
– Fluid collection	100(75.3–100)	30.0(6.7–65.2)	65.0(40.8–84.6)	100(29.2–100)	69.6(47.1–86.8)
– Contrast enhancement	92.3(64.0–99.8)	50.0(18.7–81.3)	83.3(35.9–99.6)	70.6(44.0–89.7)	73.9(51.6–89.8)
– Gas formations	23.1(5.0–53.8)	90.0(55.5–99.7)	47.4(24.4–71.1)	75.0(19.4–99.4)	52.2(30.6–73.2)
– All four findings present	23.1(5.0–53.8)	100(69.2–100)	50.0(27.2–72.8)	100(29.2–100)	56.5(34.5–76.8)
Combined CE-PET/CT					
Reader 1 overall	100(75.3–100)	70.0(34.8–93.3)	100(59.0–100)	81.3(54.4–96.0)	86.9(66.4–97.2)
– If confident	100(75.3–100)	50.0(6.8–93.2)	100(15.8–100)	86.7(59.5–98.3)	88.2(63.6–98.5)
– If not confident	n.a.	n.a	n.a	n.a	n.a
Reader 2 overall	100(75.3–100)	80.0 (44.4–97.5)	100(63.1–100)	86.7(59.5–98.3)	91.3(71.9–98.9)
– If confident	100(66.4–100)	83.3 (35.9–99.6)	100(47.8–100)	90.0(55.5–99.7)	93.3(68.1–99.8)
– If not confident	100(39.8–100)	75.0 (19.4–99.4)	100(29.2–100)	80.0(28.4–99.5)	87.5(47.4–99.7)

PET/CT: positron emission tomography/computed tomography; CE: contrast-enhanced; CT: computed tomography; CI: confidence interval; SUV$_{max.}$: maximum standardized uptake value; NPV: negative predictive value; PPV: positive predictive value; n.a.: not applicable

Strengths and limitations of the study

Strengths of the current study are its prospective design, the clinical and imaging follow-up of patients with and without VGI, and the multidisciplinary team approach. As in other cohorts of patients with VGI emergency PET/CT imaging before surgery was difficult to perform and therefore PET/CT was often acquired only after a first surgical revision. We excluded

Fig. 4 In the same patient as in Fig. 3, all readers of PET/CT, CE-CT, and combined CE-PET/CT correctly described spondylodiscitis as an incidental finding as displayed on sagittal reconstructed fused PET/CT (**a**) and CE-CT images (**b**)
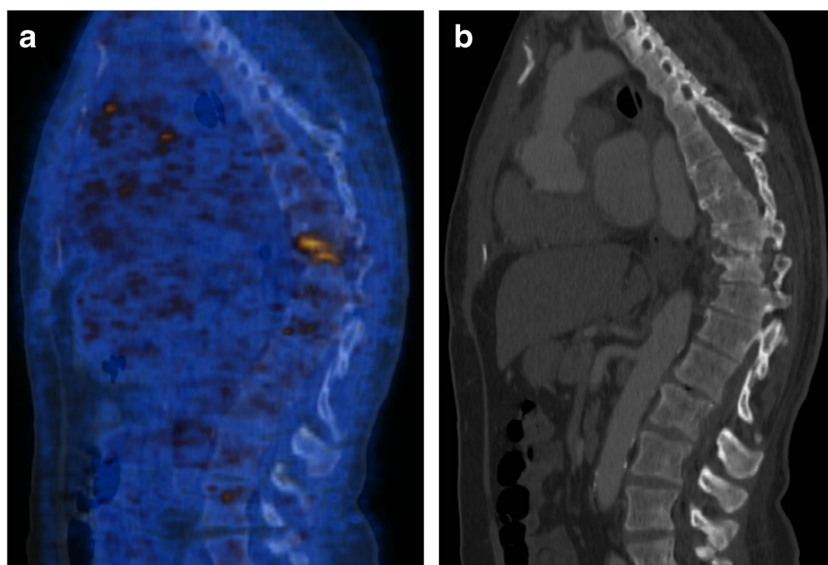
PET/CT results obtained after surgical revisions and/or > 3 months after VGI diagnosis to avoid bias, which resulted in the exclusion of a considerable number of patients (61%) for this study. In comparison to previous publications [6–9], we successfully reduced the percentage of patients receiving antimicrobial treatment or surgery prior to imaging, as it has been discussed to potentially lower the sensitivity and/or specificity of imaging procedures. However, in the present study we did not detect any false negative findings with combined CE-PET/CT. Therefore, one may conclude, that the impact of antibiotic treatment on diagnostic accuracy in VGI might be negligible, and a possible delay of antimicrobial treatment in patients with less severe clinical presentation is neither useful nor recommendable. The latter is in line with recent publications, stating that antimicrobial treatment does not impair the diagnostic accuracy of PET/CT in the evaluation of known or suspected infectious processes in general [21]. Differences in diagnostic accuracies as described above were statistically not significant. Therefore, further studies are needed to confirm our results.

Conclusion

The diagnostic accuracy of combined CE-PET/CT in patients with suspected VGI is very high. The combination of the high sensitivity of PET/CT in detecting metabolically active infectious foci and the high specificity of CE-CT in detecting anatomic alterations, appears to be the reason why combined imaging outperforms stand-alone imaging in diagnosing VGI.

Compliance with ethical standards

References

1. Hallett JW Jr, Marshall DM, Petterson TM, et al. Graft-related complications after abdominal aortic aneurysm repair: reassurance from a 36-year population-based experience. J Vasc Surg. 1997;25(2):277–84 discussion 285–286.

2. Wilson WR, Bower TC, Creager MA, et al. Vascular graft infections, mycotic aneurysms, and endovascular infections: a scientific statement from the American Heart Association. Circulation. 2016;134(20):e412–e60.

3. Hasse B, Husmann L, Zinkernagel A, Weber R, Lachat M, Mayer D. Vascular graft infections. Swiss Med Wkly. 2013;143:w13754.

4. Keidar Z, Nitecki S. FDG-PET in prosthetic graft infections. Semin Nucl Med. 2013;43(5):396–402.

5. Lyons OT, Baguneid M, Barwick TD, et al. Diagnosis of aortic graft infection: a case definition by the Management of Aortic Graft Infection Collaboration (MAGIC). Eur J Vasc Endovasc Surg. 2016;52(6):758–63.

6. Fukuchi K, Ishida Y, Higashi M, et al. Detection of aortic graft infection by fluorodeoxyglucose positron emission tomography: comparison with computed tomographic findings. J Vasc Surg. 2005;42(5):919–25.

7. Keidar Z, Engel A, Hoffman A, Israel O, Nitecki S. Prosthetic vascular graft infection: the role of 18F-FDG PET/CT. J Nucl Med. 2007;48(8):1230–6.

8. Spacek M, Belohlavek O, Votrubova J, Sebesta P, Stadler P. Diagnostics of "non-acute" vascular prosthesis infection using 18F-FDG PET/CT: our experience with 96 prostheses. Eur J Nucl Med Mol Imaging. 2009;36(5):850–8.

9. Bruggink JL, Glaudemans AW, Saleem BR, et al. Accuracy of FDG-PET-CT in the diagnostic work-up of vascular prosthetic graft infection. Eur J Vasc Endovasc Surg. 2010;40(3):348–54.

10. Sah BR, Husmann L, Mayer D, et al. Diagnostic performance of F-FDG-PET/CT in vascular graft infections. Eur J Vasc Endovasc Surg 2015;49(4):455–64.

11. Tokuda Y, Oshima H, Araki Y, et al. Detection of thoracic aortic prosthetic graft infection with 18F-fluorodeoxyglucose positron emission tomography/computed tomography. Eur J Cardiothorac Surg. 2013;43(6):1183–7.

12. Stumpe KD, Dazzi H, Schaffner A, von Schulthess GK. Infection imaging using whole-body FDG-PET. Eur J Nucl Med. 2000;27(7):822–32.

13. Low RN, Wall SD, Jeffrey RB Jr, Sollitto RA, Reilly LM, Tierney LM Jr. Aortoenteric fistula and perigraft infection: evaluation with CT. Radiology. 1990;175(1):157–62.

14. Bruggink JL, Slart RH, Pol JA, Reijnen MM, Zeebregts CJ. Current role of imaging in diagnosing aortic graft infections. Semin Vasc Surg. 2011;24(4):182–90.

15. Keidar Z, Pirmisashvili N, Leiderman M, Nitecki S, Israel O. 18F-FDG uptake in noninfected prosthetic vascular grafts: incidence, patterns, and changes over time. J Nucl Med. 2014;55(3):392–5.

16. Husmann L, Hasse B. PET-CT in vascular graft infections. Zentralbl Chir. 2017;142(5):502–5.

17. Pfannenberg AC, Aschoff P, Brechtel K, et al. Value of contrast-enhanced multiphase CT in combined PET/CT protocols for oncological imaging. Br J Radiol. 2007;80(954):437–45.

18. Saleem BR, Berger P, Vaartjes I, et al. Modest utility of quantitative measures in F-fluorodeoxyglucose positron emission tomography scanning for the diagnosis of aortic prosthetic graft infection. J Vasc Surg 2014;61(4):965–71.

19. Cheson BD, Fisher RI, Barrington SF, et al. Recommendations for initial evaluation, staging, and response assessment of Hodgkin and non-Hodgkin lymphoma: the Lugano classification. J Clin Oncol. 2014;32(27):3059–68.

20. Pizzi MN, Roque A, Fernandez-Hidalgo N, et al. Improving the diagnosis of infective endocarditis in prosthetic valves and Intracardiac devices with 18F-Fluordeoxyglucose positron emission tomography/computed tomography angiography: initial results at an infective endocarditis referral center. Circulation. 2015;132(12):1113–26.

21. Kagna O, Kurash M, Ghanem-Zouabi N, Keidar Z, Israel O. Does antibiotic treatment affect the diagnostic accuracy of FDG PET/CT studies in patients with suspected infectious processes? J Nucl Med. 2017;58(11):1827–1830.